Environmental Research 217 (2023) 114836

Contents lists available at ScienceDirect

Environmental Research

journal homepage: www.elsevier.com/locate/envres

Binding of common organic UV-filters to the thyroid hormone transport protein transthyretin using *in vitro* and *in silico* studies: Potential implications in health.

Ellen Y. Cotrina [a], Ângela Oliveira [b], Jordi Llop [c], Jordi Quintana [e], Xevi Biarnés [f], Isabel Cardoso [b,d,**], M. Silvia Díaz-Cruz [g,***], Gemma Arsequell [a,*]

[a] *Institut de Química Avançada de Catalunya (IQAC), Spanish Council of Scientific Research (IQAC-CSIC), 08034, Barcelona, Spain*
[b] *Molecular Neurobiology Group, I3S - Instituto de Investigação e Inovação Em Saúde, IBMC - Instituto de Biologia Molecular e Celular, Universidade Do Porto, Rua Alfredo Allen 208, 4200-135, Porto, Portugal*
[c] *CIC BiomaGUNE, Basque Research and Technology Alliance (BRTA), 20014, San Sebastian, Spain*
[d] *Instituto de Ciências Biomédicas Abel Salazar (ICBAS), 4050-013, Porto, Portugal*
[e] *Research Programme on Biomedical Informatics, Universitat Pompeu Fabra (UPF-IMIM), 08003, Barcelona, Spain*
[f] *Laboratory of Biochemistry, Institut Químic de Sarrià, Universitat Ramon Llull (URL), 08017, Barcelona, Spain*
[g] *ENFOCHEM Group. Institute of Environmental Assessment and Water Research (IDÆA) Excellence Center Severo Ochoa, Spanish Council of Scientific Research (CSIC), 08034, Barcelona, Spain*

ARTICLE INFO

Keywords:
UV-Filters
Parabens
Sunscreens
Transthyretin-binders
Transthyretin mediated transport
Endocrine disrupting compounds
Transplacental transport

ABSTRACT

Several anthropogenic contaminants have been identified as competing with the thyroid hormone thyroxine (T_4) for binding to transport proteins as transthyretin (TTR). This binding can potentially create toxicity mechanisms posing a threat to human health. Many organic UV filters (UVFs) and paraben preservatives (PBs), widely used in personal care products, are chemicals of emerging concern due to their adverse effects as potential thyroid-disrupting compounds. Recently, organic UVFs have been found in paired maternal and fetal samples and PBs have been detected in placenta, which opens the possibility of the involvement of TTR in the transfer of these chemicals across physiological barriers. We aimed to investigate a discrete set of organic UVFs and PBs to identify novel TTR binders. The binding affinities of target UVFs towards TTR were evaluated using *in vitro* T_4 competitive binding assays. The ligand-TTR affinities were determined by isothermal titration calorimetry (ITC) and compared with known TTR ligands. In parallel, computational studies were used to predict the 3-D structures of the binding modes of these chemicals to TTR. Some organic UVFs, compounds 2,2′,4,4′-tetrahydroxybenzophenone (BP2, Kd = 0.43 μM); 2,4-dihydroxybenzophenone (BP1, Kd = 0.60 μM); 4,4′-dihydroxybenzophenone (4DHB, Kd = 0.83 μM), and 4-hydroxybenzophenone (4HB, Kd = 0.93 μM), were found to display a high affinity to TTR, being BP2 the strongest TTR binder (ΔH = −14.93 Kcal/mol). Finally, a correlation was found between the experimental ITC data and the TTR-ligand docking scores obtained by computational studies. The approach integrating *in vitro* assays and *in silico* methods constituted a useful tool to find TTR binders among common organic UVFs. Further studies on the involvement of the transporter protein TTR in assisting the transplacental transfer of these chemicals across physiological barriers and the long-term consequences of prenatal exposure to them should be pursued.

Abbreviations: BBB, Blood Brain Barrier; BP, benzophenone; BT, benzotriazole; DMSO, dimethyl sulfoxide; EHMC, 2-ethyl-hexyl-4-methoxycinnamate; HEPES, *N*-(2-hydroxyethyl)piperazine-*N*′-(2-ethanesulfonic acid); HPLC-HRMS, High Performance Liquid Chromatography coupled to High Resolution Mass Spectrometry; HSA, Human Serum Albumin; IDIF, Iododiflunisal; ITC, Isothermal Titration Calorimetry; NMR, Nuclear Magnetic Resonance; OC, octocrylene; PAGE, polyacrylamide gel electrophoresis; PB, paraben; RBP, Retinol Binding Protein; RT, room temperature; TBG, Thyroxine-Binding Globulin; T_4, thyroxine; Tris, *tris* (hydroxymethyl-aminomethane; TTR, Transthyretin; UV, Ultraviolet; UVFs, UV filters; WHO, World Health Organization; wt, wild-type.

* Corresponding author.
** Corresponding author.
*** Corresponding author.
E-mail addresses: icardoso@ibmc.up.pt (I. Cardoso), silvia.diaz@idaea.csic.es (M.S. Díaz-Cruz), gemma.arsequell@iqac.csic.es (G. Arsequell).

https://doi.org/10.1016/j.envres.2022.114836
Received 20 September 2022; Received in revised form 3 November 2022; Accepted 14 November 2022
Available online 17 November 2022

1. Introduction

Ultraviolet (UV) radiation is considered a public health threat because UV radiation exposure can promote skin cancer (World Health Organization, 2022). The increasing awareness of consumers regarding the effects of exposure to UV rays has fueled the production of sunscreen products (BCC research, 2022). The most important ingredients in sunscreens are organic and inorganic UV filters (UVFs) (Shaath, 2010). Organic UVFs are present in increasing amounts not only in personal care and hygiene products (*e.g.* cosmetics, hair-care, after shave lotions, etc.), but also in certain materials (plastics, textiles, and paints, among others) (Sabzevari et al., 2021). The large global production of these chemicals, together with their continuous release, poor degradability, and lipophilicity, have resulted in their widespread environmental occurrence and persistence worldwide (OffEur and Union, 2009).

Organic UVFs have been extensively detected in aquatic ecosystems (Díaz-Cruz and Barceló, 2015) including biota such as corals (Tsui et al., 2017), jellyfish (Bell et al., 2017), fish (Molins-Delgado et al., 2018a), bird eggs (Molins-Delgado et al., 2017), and marine mammals like dolphins (Alonso et al., 2015). Organic UVFs have also been detected in humans; in the brain white matter (van der Meer et al., 2017), in urine (Ao et al., 2018), in breast milk (Molins-Delgado et al., 2018b), in placenta (Valle-Sistac et al., 2016), in umbilical cord (Sunyer-Caldú et al., 2021), and in amniotic fluid (Krause et al., 2018). Their presence in paired maternal and fetal samples (Krause et al., 2018; Song et al., 2020) indicates that pregnant women and their fetuses accumulate and transfer UVFs after exposure. Notably, the occurrence of these chemicals in the brain and in umbilical cord blood indicates that these compounds can cross physiological barriers such as the blood-brain barrier (BBB) (van der Meer et al., 2017; Pomierny et al., 2019) and the placental barrier (Koren and Ornoy, 2018), respectively. Hence, transport proteins in these barriers may play a critical role in their transfer process.

Human Transthyretin (TTR), together with thyroxine-binding globulin (TBG), and albumin (HSA), is one of the three main thyroid hormone transport proteins in plasma. TTR is a human homotetrameric protein (55 KDa) that is synthesized both in the liver and in the choroid plexus and circulates in blood and cerebrospinal fluid (Vieira and Saraiva, 2014). In addition, TTR is also secreted by placental trophoblasts which are critical to normal fetal development (McKinnon et al., 2005). The role of TTR as a transporter protein is singularly relevant as TTR can cross both the placental and blood brain barriers (Vieira and Saraiva, 2014). TTR appears to play an important function in the transfer of maternal thyroid hormone to the fetal circulation (Landers et al., 2013).

So far, several environmental contaminants have been identified as TTR binders competing with T_4 for binding, diverse chemicals such as tetrabromobisphenol A (Iakovleva et al., 2016), polychlorinated biphenyls (Purkey et al., 2004; Marchesini et al., 2006, 2008), perfluoroalkyl compounds (Weiss et al., 2009; Ren et al., 2016; Xin et al., 2018), polybrominated diphenyl ethers (Marchesini et al., 2008; Ren and Guo, 2012; Hill et al., 2018a), and house dust contaminants (Zhang et al., 2015, 2016; Hamers et al., 2020). Interestingly, an *in silico* approach was developed by Zhang et al. (2015) to evaluate the potential toxicity of chemicals having TTR as the molecular target. Among TTR binders, these authors reported the presence of 2,2′,4,4′-tetrahydroxybenzophenone (BP2) while the binary complex BP2/TTR was also later reported by the abovementioned (Zhang et al., 2016), showing the specific interactions with TTR at molecular level.

The binding of these anthropogenic contaminants to TTR can potentially create mechanisms of toxicity and pose a threat to human health. Many UVFs have been identified as endocrine disruptors (de Miranda et al., 2021) and have been associated with other health effects (Kunisue et al., 2012; Teiri et al., 2021).

In human blood, only about 15% of thyroxine (T_4) is transported by TTR, suggesting that this competitive binding in the blood may be an etiological process that may manifest adverse effects caused by these chemicals. This toxicological etiology may have a larger toxicological role in fetal tissues and cerebrospinal fluid in the brain, where TTR is the main T_4 carrier, transporting about 80% of the hormone (Bezerra et al., 2020). In adult mammals, only 0.5% hematological TTR circulation is occupied by T_4 (Pappa and Refetoff, 2017). TTR is a carrier of other compounds that have binding sites that do not compete with the T_4 binding site (Richardson, 2009). Thus, TTR may bind and transport these xenobiotic compounds to different tissues, causing adverse health effects. Remarkably, another potentially harmful consequence of the chronic exposure to these chemicals stems from the fact that TTR can cross the placental barrier and the BBB, allowing these compounds to surpass these physiological barriers and hence, accumulating in vulnerable organs as suggested by Song et al. (Song et al., 2020; Hamers et al., 2020; Wang et al., 2021). In a previous study, we documented that the formation of a binary complex between TTR and the small-molecule iododiflunisal (IDIF) enhances BBB's permeability of both the ligand IDIF and the TTR in the brain (Ríos et al., 2019), and may represent an important mechanism behind major adverse effects in humans, after chronic exposure, for both the fetus and the pregnant women.

In the present work, aiming to identify novel TTR binders, we investigated a discrete set of extensively produced organic UVFs and PB preservatives which are commonly used in beauty and hygiene products and detected in the environment and in human matrices such as the brain and placenta (Valle-Sistac et al., 2016; van der Meer et al., 2017; Pomierny et al., 2019). In addition, we aimed to find an approach to predict the potency of binding modes of TTR ligands by computational studies. Their TTR binding capacities have been evaluated using *in vitro* competitive binding assays. To gain further knowledge at the molecular level, the ligand/TTR binding affinities of 15 compounds (See Fig. 1) were studied by Isothermal Titration Calorimetry (ITC), and the thermodynamic profile of the best TTR binder was determined. Additionally, computational docking was used to predict the 3-D structures of the binding modes of these chemicals to TTR.

2. Materials and methods

2.1. A stepwise method's protocol was developed

(1) Evaluating whether the compounds under study bind to TTR by two different T_4 binding assays. (a) A qualitative assay of T_4 binding by gel electrophoresis using human plasma as TTR's source with a selection of the target compounds. (b) A T_4 binding competition assay with the selected compounds for the determination of their EC_{50} values and the corresponding relative binding potency in comparison with T_4. (2) Investigating the TTR binding affinities by ITC studies and determining the thermodynamic profile of the best TTR binders, and (3) Computational docking application to predict the 3-D structures of the binding modes of these chemicals to TTR.

2.2. Chemicals

HEPES, *N*-(2-Hydroxyethyl) piperazine-*N*′-(2-ethanesulfonic acid); Glycine; Tris (*Tris*(hydroxymethyl)-aminomethane); Dimethyl sulfoxide (DMSO) were supplied by Sigma-Aldrich. The radioligand ^{125}I-T_4 (specific radioactivity ≈1200 μCi/μg; concentration 320 mCi/mL) was obtained from PerkinElmer (USA). All the chemicals used in these assays were purchased from Sigma-Aldrich (Darmstadt, Germany) (for specific additional information such as the CAS number, the suppliers' reference number and the purity of these chemicals, see Table S1 at the Supplementary Material). The purity of all commercially available compounds as specified by the supplier was ≥98%. The registered drugs Diflunisal (2′,4′-difluoro-4-hydroxy-[1,1′-biphenyl]-3-carboxylic acid) and Tolcapone (3,4-dihydroxy-4′-methyl-5-nitrobenzophenone) were commercially available (≥98% HPLC, Darmstadt, Sigma-Aldrich).

We followed reported procedures in the literature (Razavi et al., 2003) for the synthesis of Tafamidis (2-(3,5-dichlorophenyl)-1,3-benzoxazole-6-carboxylic acid) in our laboratory. Our small-molecule

ligand IDIF (2′,4′-difluoro-4-hydroxy-5-iodo-[1,1′-biphenyl]-3-carboxylic acid) was prepared following our previously described procedure (Mairal et al., 2009). Purity of final compounds was ≥95% calculated by means of high-performance liquid chromatography coupled to high resolution mass spectrometry (HPLC-HRMS) and NMR techniques.

2.3. TTR production and purification

The production of recombinant protein was performed at Erlenmeyer scale; protein production and purification were carried out following an optimized version of the protocol (Cotrina et al., 2020a). wtTTR was produced using a pET expression system. The expressed protein only contains an additional methionine on the N-terminus if compared to the mature natural human protein sequence. wtTTR protein was expressed in *E. coli* BL21-(DE3) cells harboring the corresponding plasmid. Expression cultures in 2xYT rich medium containing 100 μg/mL kanamycin were grown at 37 °C to an optical density (at 600 nm) of 4 (OD600 ≈ 4), then induced by addition of IPTG (1 mM final concentration), grown at 37 °C for 20 h, and harvested by centrifugation at 4 °C, 10,000 rpm for 10 min and resuspended in cell lysis buffer (0,5 M Tris-HCl, pH 7.6). Cell disruption and lysis were performed by French press followed by a sonication step at 4 °C. Cell debris were discarded after centrifugation at 4 °C, 11,000 rpm for 30 min. Intracellular proteins were fractionated by ammonium sulfate precipitation in three steps. Each precipitation was followed by centrifugation at 12 °C, 12, 500 rpm for 30 min. The pellets were analyzed by SDS-PAGE (14% acrylamide). The TTR-containing fractions were resuspended in 20 mM Tris-HCl, 0.1 M NaCl, pH 7.6 (buffer A) and dialyzed against the same buffer. It was purified by ion exchange chromatography using a Q-Sepharose High Performance (Amersham Biosciences) anion exchange column and eluted with a NaCl linear gradient using 0.1 M NaCl in 20 mM Tris-HCl pH 7.6 buffer A to 0.5 M NaCl 20 mM Tris-HCl pH 7.6 (buffer B). All TTR-enriched fractions were dialyzed against deionized water in three steps and they were lyophilized afterwards. The protein was further purified by gel filtration chromatography using a Superdex 75 prep grade resin (GE Healthcare Bio-Sciences AB) and eluted with 20 mM Tris pH 7.6, 0.1 M NaCl. Purest fractions were combined and dialyzed against deionized water and lyophilized. The purity of protein preparations was >95% as judged by SDS-PAGE. Protein concentration was determined by the Bradford Method (Bio-Rad), using bovine serum albumin as standard (Bradford, 1976). The protein was stored at −20 °C.

2.4. Thyroxine (T_4) binding assays

2.4.1. Qualitative assay of T_4 binding by gel electrophoresis

We have first performed a qualitative assay that uses radiolabeled T_4 and plasma as source of TTR to evaluate whether a compound binds to TTR or not. The ability of the selected compounds to displace T_4 and their specificity for TTR binding was evaluated. A decrease in the intensity of the [^{125}I]-T_4/TTR band was observed if a ligand binds to TTR in the T_4 central binding channel. In addition, this qualitative assay also revealed the specificity for TTR binding for each ligand.

We followed a previously described method (Cotrina et al., 2021) to perform the qualitative assay. Displacement of T_4 from plasma TTR (*ex vivo*) was first analyzed by native polyacrylamide gel electrophoresis (PAGE) after incubation of 15 μL of a mixture of 5 μL human plasma (5 μL) with 0.25 μL ^{125}I-T_4 (specific radioactivity ≈1200 μCi/μg; concentration 320 mCi/mL; PerkinElmer) and buffer in the presence of 1 μL of a 10 mM solution of the small-molecules (final concentration, 667 μM). As for the negative control, 1 μL of PBS was added. The samples were incubated for 1h at RT. After incubation, the different plasma T_4 binding proteins from human plasma, *i.e.* TTR, TBG and HSA, were separated by native PAGE system using an 8% acrylamide and glycine/acetate resolving gel. The gels were dried and revealed using an X-ray film. The three observed bands correspond to proteins TBG, HSA and TTR, which are three-major T_4-binding plasma proteins, being TTR the one presenting the most anodal migration. Those compounds found to bind to TTR in this qualitative assay were selected for a second quantitative assay.

2.4.2. T_4 binding competition assay

A previously described radiolabeled ligand competition assay was followed (Almeida et al., 2000; Cotrina et al., 2021). This is one of the most conventional methods and uses radiolabeled T_4 as the radiotracer in the competitive binding assay. The competitive binding was carried out to measure the binding ability of T_4 and other compounds with TTR. This ^{125}I-T_4 binding competition assay was based on a gel filtration procedure. Briefly, 30 nM recombinant human wtTTR was incubated with cold T_4 or compound solutions of variable concentrations ranging from 0 to 1000 nM and with a constant amount of labeled ^{125}I-T_4 (~50, 000 cpm). This solution was counted in a gamma spectrometer and incubated at 4 °C overnight. Protein bound ^{125}I-T_4 and free ^{125}I-T_4 were separated by gel filtration through a 1 mL BioGel P6DG (Bio-Rad) column. The bound fraction was eluted, while free ^{125}I-T_4 was retained on the BioGel matrix. The eluate containing the bound ^{125}I-T_4 was collected and counted. Bound ^{125}I-T_4 was expressed as percentage of total ^{125}I-T_4 added. Each assay was performed in duplicate. Analysis of the binding data was performed with the GraphPad Prism program (V. 9.0, San Diego, CA, USA). Percentage binding was plotted against the logarithm of the inhibitor concentration, and the EC_{50} for a compound (concentration that is capable of replacing 50% of a labeled TTR ligand from TTR) was determined and compared with the EC_{50} for T_4 (used as positive control). The [EC_{50} ^{125}I-T_4/EC_{50} compound] ratio is the relative inhibition potency and by definition, when the ligand is T_4, the ratio is 1. Thus, compounds with higher affinity for TTR than the natural ligand have a ratio >1, and compounds with a ratio <1 have lower affinity for TTR.

2.5. Isothermal titration calorimetry (ITC)

An VP-ITC equipment (MicroCal, LLC, Northampton, Ma, USA) was used for ITC measurements. We followed our previously described methods (Cotrina et al., 2020b, 2021). At the beginning of the experiment the calorimetric cell is filled with a TTR solution in buffer, with an effective volume that is calorimetrically sensed. In a titration experiment, a solution of the compound in the syringe is added in small aliquots to the calorimeter cell. The stock solutions of the small-molecule compounds were prepared in DMSO. All solutions, either protein or compounds, were prepared in 25 mM HEPES buffer, 10 mM glycine at pH 7.4 and 5% DMSO (as final concentration). The concentrations of TTR solutions were 5–10 μM and 50–100 μM for ligand solutions. All solutions were filtered and degassed prior to usage. The TTR protein solution was injected over 20 or 30 times, at a constant interval of 300 s and 450 rpm rotating stirrer syringe into the sample cell.

In the control experiment, the ligand was injected into the buffer in the sample cell to obtain the dilution's heat. The obtained value was subtracted from the experimental result in the final analysis. Experiments were performed at 25 °C, and reference power at 10. Titration data were analyzed by the MicroCal Origin, V.7.0 software provided by the manufacturer. The binding curves were fitted to the calculations of the parameters binding stoichiometry (N), dissociation constant (K_d), and the changes in the enthalpy (ΔH), entropy (ΔS) and Gibbs free energy (ΔG) during the complex formation. Each experiment was carried out in triplicate and the mean values with standard deviations are provided. Data were obtained from the adjustment of the ITC curves with binding equations available in the Origin software (identical and independent binding sites or sequential sites).

2.6. Biomolecular visualization

The structures of TTR's binary complexes with diverse ligands can be accessed in the RCSB Protein Data Bank (PDB) (https://www.rcsb.org/pdb). Three 3D structures of human TTR complexes from X-ray crystallography were taken as a reference. One in complex with the endogenous ligand thyroxine (T_4) (PDB code: 1ICT) (Wojtczak et al., 2001), and two complexes with other relevant ligands: 2,2′,4,4′-tetrahydroxybenzophenone (BP2) (PDB code: 5JIQ), and the repurposed drug Tolcapone (PDB code: 4D7B). Compounds BP2 and Tolcapone, share a benzophenone-type (BP-type) scaffold. The visualizations were prepared based on these three structures and were performed using the Visual Molecular Dynamics (VMD V.1.9.1) software (Humphrey et al., 1996). The protein-ligand interactions were measured at the binding site, defined as the list of amino acids with at least one atom within 5 Å of any of the ligand atoms.

2.7. Computational docking calculations

To reveal underlying interaction mechanisms between model compounds and TTR, molecular modeling was used. The 3D structures of the ligands shown in Figs. 4 and 5 were generated with the MOE software, from Chemical Computing Group (Molecular Operating Environment, 2019). The addition of polar hydrogens and Gasteiger charges was performed using AutoDock 4.2 and its graphical front-end AutoDock Tools (Morris et al., 2009). All non-aromatic and non-amide bonds were defined as rotatable. For the TTR protein (PDB 1ICT), all water molecules were removed, Gasteiger charges were computed, and solvation parameters were added. All protein sidechains were defined as rigid. The grid box size was defined to provide big enough search space for all ligands to be docked. The number of points in *x*-, y- and z-dimensions of the grid box was 70 × 50 × 70 points and the grid-point spacing was 0.375 Å/point. The center of mass of thyroxine ligand co-crystallized with TTR receptor (PDB 1ICT) was used as mid-point of the grid box. To perform docking calculations the Lamarckian Genetic Algorithm, as implemented in the AutoDock V. 4.2 software, was employed. For each ligand, the maximum numbers of energy evaluations and generations were set up to 25,000,000 and 27,000, respectively. To ensure a proper sampling of all plausible binding modes, 1000 independent docking runs were conducted for each ligand. The conformer with the lowest binding free energy was selected for further simulation analysis. AutoDock V. 4.2 software, with a root-mean square deviation (RMSD) cut-off of 0.5 Å was used to perform cluster analysis. The cut-off was 2 Å for BP4, BzPB, and BP8, because they exhibit higher population clusters. The docked conformations of each molecule were ranked into clusters based on the predicted binding energy (AutoDock V.4.2 score) and the number of occurrences. Only those conformations with a high number of occurrences and lowest binding energies were considered to obtain average binding energies from the calculated scores. Hydrogen bonding and hydrophobic interactions among docked potent binders and TTR were analyzed using the VMD V. 1.9 software (Humphrey et al., 1996).

2.8. Statistical analysis

The correlation between binding experimental free energies and computed binding affinity scores was assessed by means of linear regression following the ordinary least squares method. The goodness of the linear fit was measured via the coefficient of determination (R-squared). The data are presented as means ± SEM and were analyzed by the unpaired Student's t-test using GraphPad Prism software (V 9.0, GraphPad, San Diego, CA, USA), and those showing a p-value < 0.05 were considered significant.

3. Results and discussion

3.1. Selection of compounds

A discrete set of organic UVFs and PBs, shown in Fig. 1, were selected for this study because they are produced in large quantities, commonly used in beauty and hygiene products, and accumulate in the environment (water, soil, fauna, and flora). Among them:

Benzophenone-type (BP-type) UVFs sharing a diaryl ketone scaffold with different substitutions on their aryl rings: benzophenone-1 (BP1), benzophenone-2 (BP2), benzophenone-3 (BP3 or oxybenzone), benzophenone-4 (BP4 or sulisobenzone), 4-hydroxybenzophenone (4HB), benzophenone-8 (BP8 or dioxybenzone), 4,4′-dihydroxybenzophenone (4DHB); and benzophenone (BP) that was used as reference compound. Other UVFs: lipophilic compounds as avobenzone (AvoBP or Parsol 1789), 2-ethyl-hexyl-4-methoxycinnamate (EHMC or octinoxate); enzacamene (4-methylbenzylidene camphor, 4MBC); octocrylene (OC); and the benzotriazole UV-stabilizer: 5-methylbenzotriazole (5Me–1H-BT.

Regarding parabens, the two PB preservatives, methyl-paraben (MePB) and benzyl-paraben (BzPB), were included in the study.

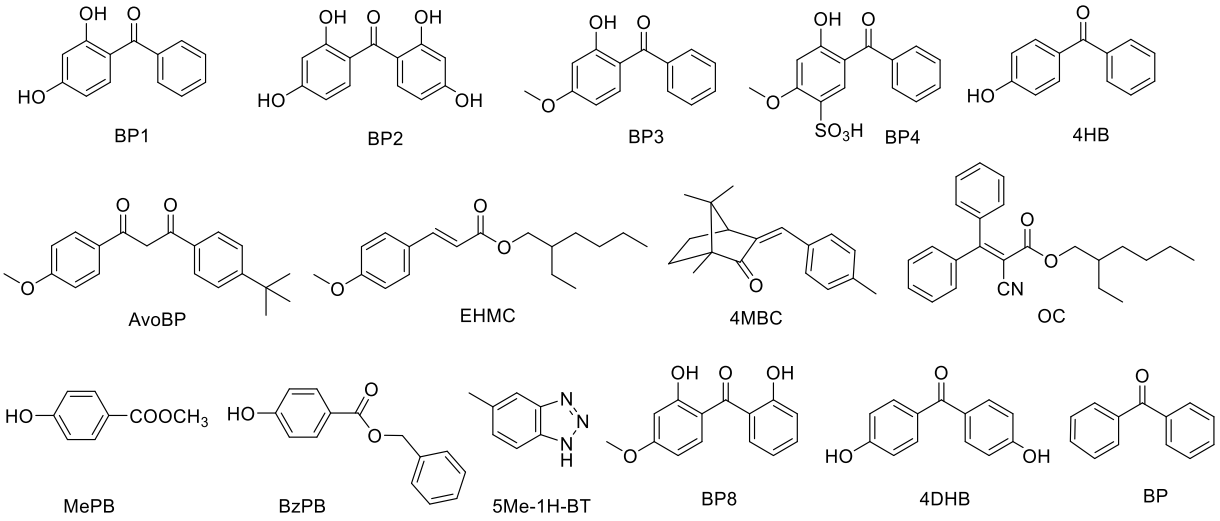

Fig. 1. Chemical structures of UVFs and PB preservatives studied (BP, benzophenone; PB, paraben; BT, benzotriazole).

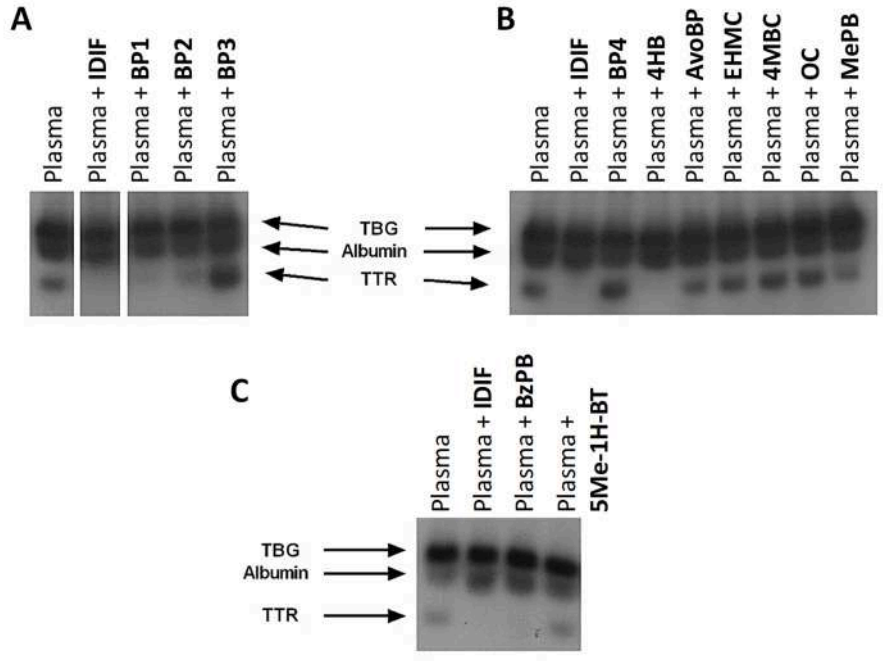

Fig. 2. T_4 displacement from TTR in human plasma. Human plasma was incubated with ^{125}I-T_4 in the presence or absence of competitors (A–C) (final concentration 667 μM). After 1h at RT, the plasma proteins (TBG, HSA and TTR) from human plasma were separated by native PAGE using 8% acrylamide native glycine/acetate resolving gel. If the TTR bound to radioactive T_4 band is not present after incubation with a compound, it indicates a selective displacement of T_4 from the TTR-binding pocket by that compound. (Uncropped images of the films for Fig. 2A are shown in Fig. S9).

3.2. Binding affinities of UVFs and PBs to wtTTR: T_4 binding assays

There are several methods to evaluate how a compound bind to TTR. Some of them use fluorescent conjugates of T_4 for those competitive assays (Ren and Guo, 2012; Ouyang et al., 2017) or use immobilized ligands for surface plasmon resonance-based biosensor assays techniques (Marchesini et al., 2006, 2008). Here, we have chosen a displacement method, which uses radiolabeled T_4 in the competitive binding assay (Lans et al., 1993; Almeida et al., 2000; Meerts et al., 2000; Weiss et al., 2015). When using plasma samples, in addition to TTR binding/stabilization, it is possible to observe how a certain compound binds not only to TTR, but also to other T_4 transporter proteins, such as TBG and HSA.

As depicted in Fig. 2, only five compounds, the BP-type UVFs (BP1, BP2, and 4HB) and the two parabens (MePB and BzPB), displaced ^{125}I-T_4 from TTR, since the intensity of the TTR/^{125}I-T_4 band was lower than the one in the absence of the compound. Moreover, the displacement of ^{125}I-T_4 from TTR in presence of BP1, 4HB and BzPB was comparable to the one by compound IDIF, a good TTR tetramer stabilizer (Mairal et al., 2009), suggesting they strongly bind to TTR. BP3, BP4, 4MBC, and OC led to the opposite effect, and their presence resulted in increased ^{125}I-T_4 binding to TTR. This binding enhancement was previously reported by Hill et al. (2018b) when studying the interaction between organophosphate triesters and TTR. These authors proposed that these allosteric interactions were a novel pathway of organophospate toxicity.

BP2 and MePB only partially displaced ^{125}I-T_4 from TTR, whereas AvoBP, EHMC, and 5Me–1H-BT did not influence TTR/^{125}I-T_4 binding.

For instance, it is possible to observe that BP1 and BP2 also bind TBG and HSA, as deduced by the slight decrease in the corresponding bands. MePB, on the other hand, binds to HSA, but not to TBG. Other compounds like BP3, showed weaker intensities for the bands corresponding to TBG and HSA, suggesting that BP3 strongly interacts with these proteins, displacing T_4. Therefore, 4HB and BzPB are the only ones that specifically bind to the TTR.

In order to characterize the binding of BP1, BP2, 4HB, MePB and BzPB, with wtTTR at the T_4 binding channel, we used competition binding studies (Almeida et al., 2000; Cotrina et al., 2021) based on a gel filtration chromatography procedure (Fig. 3), as previously described. The determination of the EC_{50} for each compound (Fig. S8) and the relative potency for the binding of a compound, defined as the ratio of the EC_{50} for T_4 by the EC_{50} for the competitor ([EC_{50} ^{125}I-T_4/EC_{50} competitor], Table 1 and Fig. 3), were performed. In this assay, AvoBP, EHMC and 4MBC were selected as negative controls according to the T_4 displacement assay results. The drug Tolcapone (Sant'Anna et al., 2016) and the compound IDIF (Mairal et al., 2009) were also employed, since they are good TTR binders (Table 1). As shown in Fig. 3 and Table 1, none of the compounds achieved higher TTR binding affinities than T_4, since none of the EC_{50} ^{125}I-T_4/EC_{50} ratios were higher than 1; as expected, IDIF displayed a high affinity towards wtTTR and an EC_{50} above 1 was determined. Therefore, although BP1, BP2, 4HB, MePB, and BzPB bind to TTR, they have a lower stabilization power than IDIF ([EC_{50} ^{125}I-T_4/EC_{50}] ratio = 1.24).

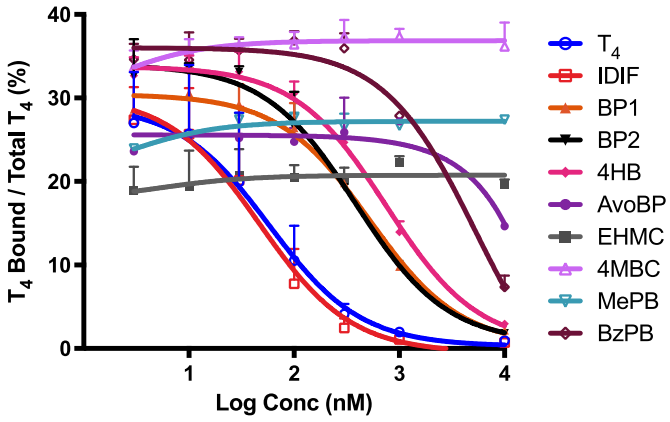

Fig. 3. Displacement of ^{125}I-T_4 from wtTTR by competition with selected compounds. Thyroxine (T_4) was used as positive control.

Table 1
Relative potency for the inhibition of T_4 binding to wtTTR.

Compound	[EC_{50} T_4/EC_{50} compound][a]
IDIF	1.24
TOLCAPONE	1.06[b]
BP1	0.12
BP2	0.18
4HB	0.09
AvoBP	–
EHMC	–
4MBC	–
MePB	–
BzPB	0.01

[a] Relative potency of competitors compared to T_4 were calculated by dividing EC_{50} (T_4) by EC_{50} (competitor).
[b] From our previous studies (Cotrina et al., 2021). Not shown in Fig. 3.

3.3. Isothermal titration calorimetry (ITC) study

We characterized the thermodynamic profiles for the binding of compounds to TTR by using ITC. The *in vitro* validation was applied to each of the 15 compounds (Fig. 1) and data was compared to four reference compounds, namely the drugs Tafamidis (Bulawa et al., 2012), Diflunisal (Cotrina et al., 2021), and Tolcapone (Sant'Anna et al., 2016), and the small-molecule compound IDIF (Mairal et al., 2009; Cotrina et al., 2021), which are known TTR tetramer stabilizers. Although the TTR tetramer can bind two ligands, it shows negative cooperative binding for the second site. Therefore, the best fitting in the ITC thermograms was obtained by using a simple one-site binding model with two identical sites.

The dissociation constants of TTR and reference compounds (IDIF, Tocalpone and Tafamidis) are in the 0.2 μM range (Table 2), with overall binding free energies around −9 kcal/mol. Compounds with Kd < 1.5 μM are considered to be good binders (the reference ligand Diflunisal has a Kd = 0.90 μM). Among the 15 ligands under investigation, those showing strongest TTR affinities are: BP1, BP2, 4DHB, 4HB, and BzPB, with dissociation constants in the range 0.4 μM–1.26 μM (Table 2). The thermodynamic parameters data of these compounds show a strong enthalpic component to the overall binding affinity (ΔH = −14.93 kcal/mol for BP2) but an unfavorable entropy component (ΔS = −6.23 kcal/mol for BP2). BP3, BP4, BP8, 4MBC, MePB, and 5Me–1H-BT, exhibited a weak interaction with TTR with dissociation constants between 1.6 μM and 5.06 μM. For many of these compounds, the entropic contribution is dominant (positive ΔS) but with small binding enthalpies. Indeed, many of these compounds are either small or with limited flexibility. For the rest of compounds (AvoBP, EHMC, and OC) no interaction was detected by ITC (Fig. S2 at the Supplementary Material).

In a previous study, the thermodynamic profiles of 12 selected potential TTR binders from some dust contaminants were investigated, and 7 out of 12 representative compounds (such as the drug clonixin, herbicides as triclopyr, and bisphenol S, among others) had binding affinities (Kd values) between 0.26 and 100 μM (Zhang et al., 2016). In our study, the UVFs analyzed by ITC have Kd values between 0.43 and 5 μM, and among the binders, we have identified a discrete set of BP-type UVFs, together with the two PBs and a benzotriazole derivative. Among the BP-type UVFs, BP1 and BP2 revealed as very good binders. Among the two PBs, it is interesting to note that the compound with the lower Kd is BzPB (Kd = 1.26 μM) which has a larger structure, higher lipophilicity (log Kow = 3.4), and lower water solubility (0.15 g/L, 25 °C) in comparison with MePB. Interestingly, our team recently reported, for the first time, the occurrence of BP-type UVFs filters and PBs in human placenta; indeed, BzBP was the only PB detected from the four PBs studied (Valle-Sistac et al., 2016).

3.4. TTR binding site identification

The conserved binding site of TTR with BP-type compounds was identified by superimposing the 3D structures of TTR in complex with different ligands: T_4, (PDB: 1ICT), BP2 (PDB: 5JIQ) and Tolcapone (PDB: 4D7B). The ligand binding site, those amino acids within 5 Å of endogenous T_4 ligand, is composed of Met13, Lys15, Leu17, Glu54, Thr106, Ala108, Leu110, Ser115, Ser117, Thr119, and Val121 (Fig. 4). From these, the TTR positions that preserve direct polar and non-polar contacts with the rest of analyzed ligands (BP2 and Tolcapone) are Lys15, Leu17, Thr106, Ser117 and Thr119. This indicates that these five amino acids may be crucial for the binding mode of BP-type UVFs on TTR.

3.5. Structures of UVFs and PBs in complex with TTR

The 3D structure of the TTR complexes with our library of small compounds was predicted by computational docking (see Methods). Tolcapone and BP2 were included in the library as reference compounds. The docking protocol successfully reproduced the crystalline structures of TTR in complex with Tolcapone and BP2 (see Figs. S3 and S4, respectively). The root mean square differences between the predicted binding poses of the reference ligands and the corresponding crystalline structures are below 2 Å. The binding modes of BP-type UVFs and TTR is equivalent for all tested compounds and equivalent to reference binders such as T_4, Tolcapone, Tafamidis, (Fig. S5), and IDIF (Fig. 5B). For instance, the interaction between BP4 and TTR is defined by a hydrogen-bond network involving Ser117 and Thr119 of both TTR monomers, hydrophobic interactions with Leu17 and a cation-pi

Table 2
Thermodynamic parameters of the binding of compounds with TTR. Data from four reference TTR binders (IDIF, Tolcapone, Tafamidis and Diflunisal) are included. (N, binding stoichiometry; Kd, dissociation constant; ΔH, enthalpy changes; ΔH, Gibbs energy changes; and ΔS entropy changes).

Assay	N	Kd (μM)	ΔH (Kcal/mol)	TΔS (Kcal/mol)	ΔG (Kcal/mol)
TTR + IDIF	1.00 ± 0.10	0.12 ± 0.01	−12.91 ± 0.44	−3.37 ± 0.15	−9.53 ± 0.29
TTR + Tolcapone	1.89 ± 0.14	0.27 ± 0.03	−12.30 ± 0.76	−3.36 ± 0.71	−8.98 ± 0.32
TTR + Tafamidis	1.86 ± 0.15	0.20 ± 0.02	−6.57 ± 0.11	2.82 ± 0.14	−9.39 ± 0.21
TTR + Diflunisal	1.00 ± 0.12	0.90 ± 0.01	−11.96 ± 0.36	−3.70 ± 0.17	−8.25 ± 0.12
TTR + BP2	0.87 ± 0.09	0.43 ± 0.02	−14.93 ± 1.60	−6.23 ± 1.56	−8.70 ± 0.04
TTR + BP1	0,94 ± 0.11	0.60 ± 0.01	−12.04 ± 0.98	−3.53 ± 0.78	−8.51 ± 0.20
TTR + 4DHB	0.93 ± 0.12	0.83 ± 0.04	−11.32 ± 0.39	−3.00 ± 0.22	−8.31 ± 0.17
TTR + 4HB	0.87 ± 0.09	0.93 ± 0.04	−10.60 ± 0.27	−2.36 ± 0.37	−8.24 ± 0.10
TTR + BzPB	0.85 ± 0.19	1.26 ± 0.03	−9.32 ± 1.03	−1.25 ± 0.35	−8.07 ± 0.18
TTR + BP4	0.89 ± 0.12	1.63 ± 0.05	−2.42 ± 0.75	5.49 ± 0.77	−7.91 ± 0.03
TTR + BP8	0.86 ± 0.13	1.71 ± 0.01	−7.08 ± 0.85	0.67 ± 0.14	−7.74 ± 0.21
TTR + MePB	0.87 ± 0.08	1.77 ± 0.03	−3.40 ± 0.78	4.44 ± 0.69	−7.85 ± 0.09
TTR + 4MBC	0.84 ± 0.11	2.99 ± 0.07	−3.15 ± 0.17	4.38 ± 0.45	−7,53 ± 0,12
TTR + 5-Me-1H-BT	1,05 ± 0,12	3,07 ± 0,05	−2,61 ± 0,21	3,52 ± 0,18	−6.13 ± 0.14
TTR + BP	0.79 ± 0.21	3.11 ± 0.08	−5.80 ± 0.01	1.76 ± 0.29	−7.56 ± 0.31
TTR + BP3	0.84 ± 0.13	5.06 ± 0.02	−5.16 ± 1.64	2.07 ± 0.71	−7.23 ± 0.07

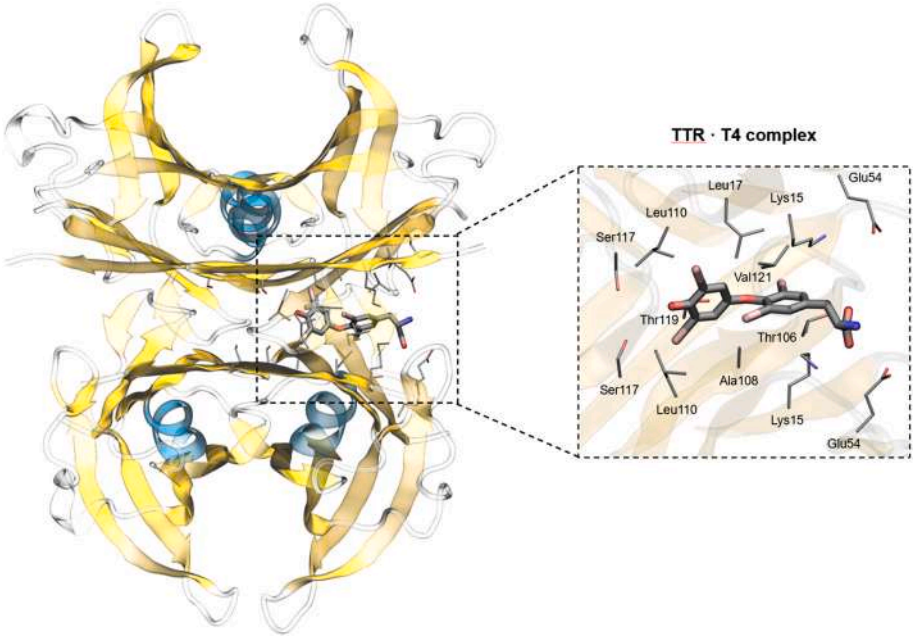

Fig. 4. Crystal structure of the wtTTR-T_4 complex (PDB: 1ICT) and magnification of the ligand binding site with the principal residues involved in TTR-ligand interactions.

interaction between the phenyl group of BP4 and Lys15 (Fig. 5A). Equivalent interactions are observed for the rest of compounds, see for instance the binding mode with the paraben BzPB (Fig. S6) and the UVF 4DHB (Fig. S7). This indicates that these compounds keep the previously identified protein-ligand interactions for analogous compounds suggesting a similar mechanism of action.

Zhang et al. (2016) performed ITC studies to characterize the binding affinities of selected compounds from dust contaminants. These authors found no correlation between the affinities of the active compounds and their corresponding docking scores. However, these researchers identified a trend, as more negative docking scores were associated with higher affinities.

The linear relationship between average predicted binding energies (AutoDock 4.2 score) and experimental ITC was determined by linear regression (Table S4 and Fig. 6). Although the correlation is not high (R^2 = 0.48) for all tested compounds, strong, high and weak binders are clearly differentiated in the correlation plot (Fig. 6), in contrast to previous studies (Zhang et al., 2016). This suggests that the molecular docking protocol used here is able to qualitatively assess the binding capacity of novel BP-like and PB compounds to TTR. We therefore propose that this TTR-ligand binding model may be used for any chemical to have a prediction of their binding energies, and thus on their possible classification as TTR strong or weak binders (Cotrina et al., 2020c).

To the best of our knowledge, the work here presented is the first comparative study of a group of extensively used organic UVFs and PBs as TTR binders. Some innovative aspects of our research are here highlighted. First, the combination of *in vitro* data from biological assays with biophysical studies to analyze and characterize the binding potential of a set of organic compounds has been assessed. ITC was selected since it is a powerful technique for the quantitative analysis of protein-ligand and protein-protein interactions, and provides a complete thermodynamic profile from a single experiment. ITC studies have been mostly used in drug discovery projects (Ward and Holdgate, 2001), but few reports can be found on the use of this innovative combination of assays in studies involving contaminants (Zhang et al., 2016; Liu et al., 2019). We have applied this combination to the study of a diverse group of largely employed UVFs.

The results presented here show that competitive displacement constitutes a useful tool to investigate the capacity to bind TTR of a collection of commonly used organic UVFs and PBs. The selected compounds bind TTR, with distinct binding potency, through the T_4 central channel, constituting a likely mechanism for the transport of such compounds across biological barriers.

Some interesting observations can be taken from those UVFs that share a common benzophenone-type scaffold (Table 2: compounds BP1, BP2, BP3, BP4, 4HB, BP8, 4DHB, and BP). The increase in the number of hydroxyl substituents in both benzophenone rings, (for instance, BP1 has only two hydroxyl groups, whereas BP2 has four) results in an increased binding affinity. Moreover, addition of a sulfonic group in *ortho* position to the methoxy group in compound BP4 compared to compound BP3; and addition of a hydroxyl in the other aromatic ring in compound BP8 compared to compound BP3, both result in increasing affinities of both compounds, BP4 and BP8, to TTR, as compared to BP3. Conversely, when some of these hydroxyl groups are substituted by methoxy groups, there is a decrease in the binding affinity. As an example, BP1 and BP3 have the same pattern of substitutions in the aromatic rings, but BP3 has one methoxy group in position 3 instead of the hydroxyl group of BP1. BP3's weakened affinity to TTR in comparison to BP1 may be explained by the lower number of potential H-bonds of BP3 with the polar residues in the T_4 binding site. Similarly, we observe a tendency for hydroxylated compounds to be better TTR binders than the corresponding methoxy-substituted compounds in the same position. The BP-type UV filter BP6 (2,2′-dihydro-4,4′-dimethoxybenzophenone), not assayed in this study, was previously reported to be a false positive TTR binder (Zhang et al., 2016). Interestingly, this compound is similar to BP2, although two methoxy groups substitute the two hydroxyl groups in 4,4′-positions of the aromatic rings of the molecule.

The possible association of BP-type UVFs exposure and health effects has been the subject of an interesting review (Mao et al., 2022). Data about BP-type UVFs transformation products and the toxicity of their metabolites is still scarce (Carstensen et al., 2022). The hydroxylated BPs obtained by these transformation processes, have a structure-related increase in endocrine activity when compared with their parent BPs, as well as a most likely increase of their binding affinities to TTR. PBs are known to display estrogenic activity in animals with increasing potency with the length of the alkyl chain. However, there are only a few human

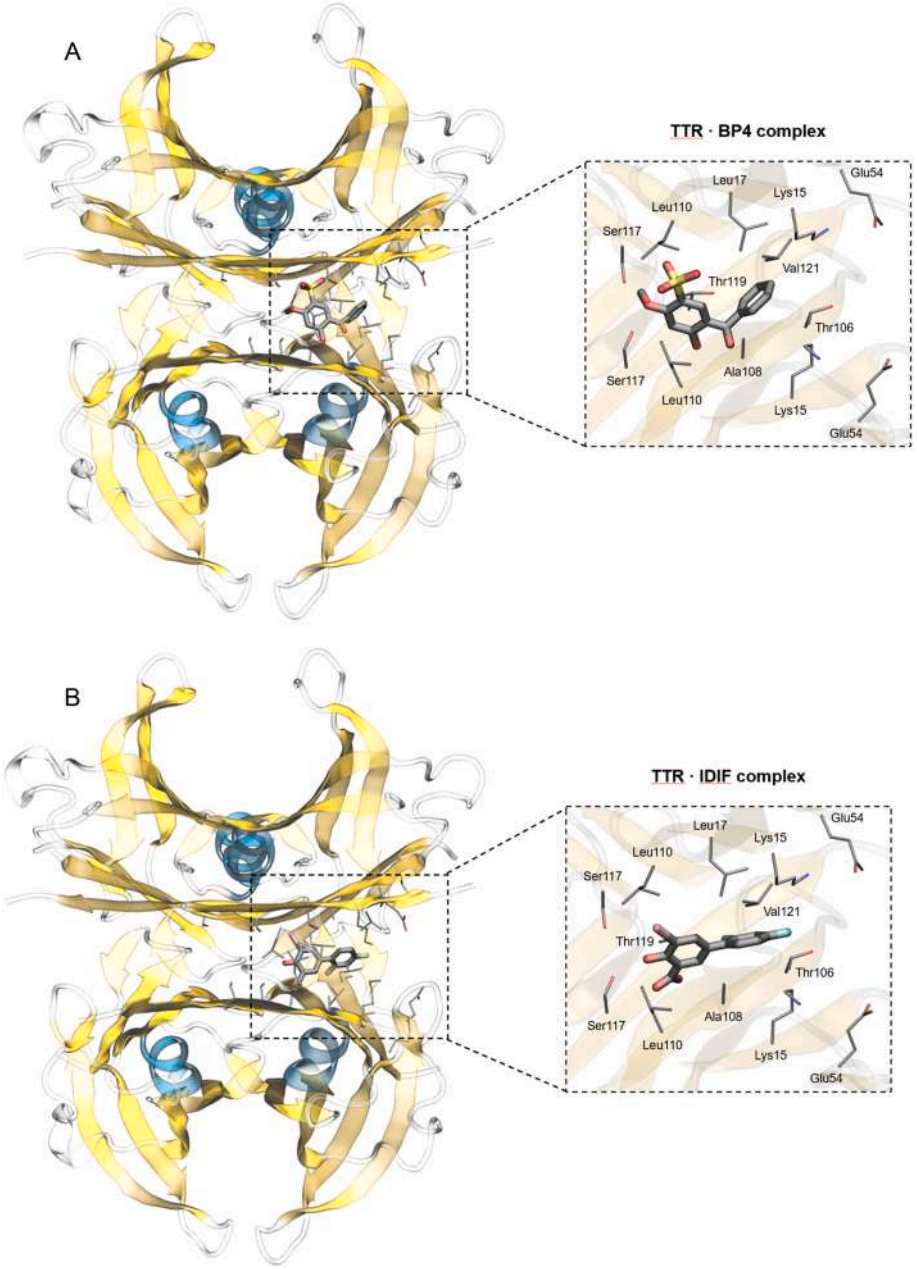

Fig. 5. Predicted 3D structures of TTR in complex with (A) BP4 and (B) IDIF showing the residues involved in the binding site.

epidemiological studies focusing on PBs, and they have linked them with allergen sensitization (Savage et al., 2012), DNA damage of sperm (Meeker et al., 2011), breast cancer and obesity (Boberg et al., 2010; Hu et al., 2013a, 2013b).

Considering the diverse physicochemical properties of all organic UVF's in use, it is difficult to experimentally estimate the TTR binding profile for all of them. The generation of new and predictive models will also prove useful to fill the data gap for other UVFs. *In silico* models are fast, cost-efficient, and powerful tools to predict the potential toxicity and decipher the action mechanisms of compounds. Only a few *in silico* models have been developed to predict the toxicity of environmental contaminants (Zhang et al., 2015). The availability of crystal structures of complexes of TTR with environmental compounds, as the one with BP2 (Zhang et al., 2016) allowed us to integrate *in vitro* data with traditional *in silico* methods such as docking studies.

We have built a model that not only allows the prediction of the TTR binding capacity of small molecules, being able to differentiate between strong, medium and non-binders to TTR, but it also provides information regarding the interactions between molecules, in this case organic UVFs and PBs with TTR.

The interactions of these daily-used chemicals with TTR can result in adverse effects by different pathways. One of the most known adverse effects results by competitively binding to the T_4 binding sites of TTR. Consequently, T_4 levels may be lower than normal, leading to an early stage of hypothyroidism, causing, if untreated, a number of health problems, such as fatigue, obesity, joint pain, infertility and heart disease. Human exposure to these chemicals can be at doses that are similar or significantly higher than the normal T_4 level (0.112 μM), or below if the compound blocks the binding sites leading to a default level of T_4 in some tissues (Huang et al., 2021; Mao et al., 2022).

On the other hand, another source of adverse effects in humans could be the TTR-mediated delivery of these compounds to other tissues, just like T_4. Even binders with low affinity to TTR could be effectively transported by TTR since most of the TTR is in the apo form in human

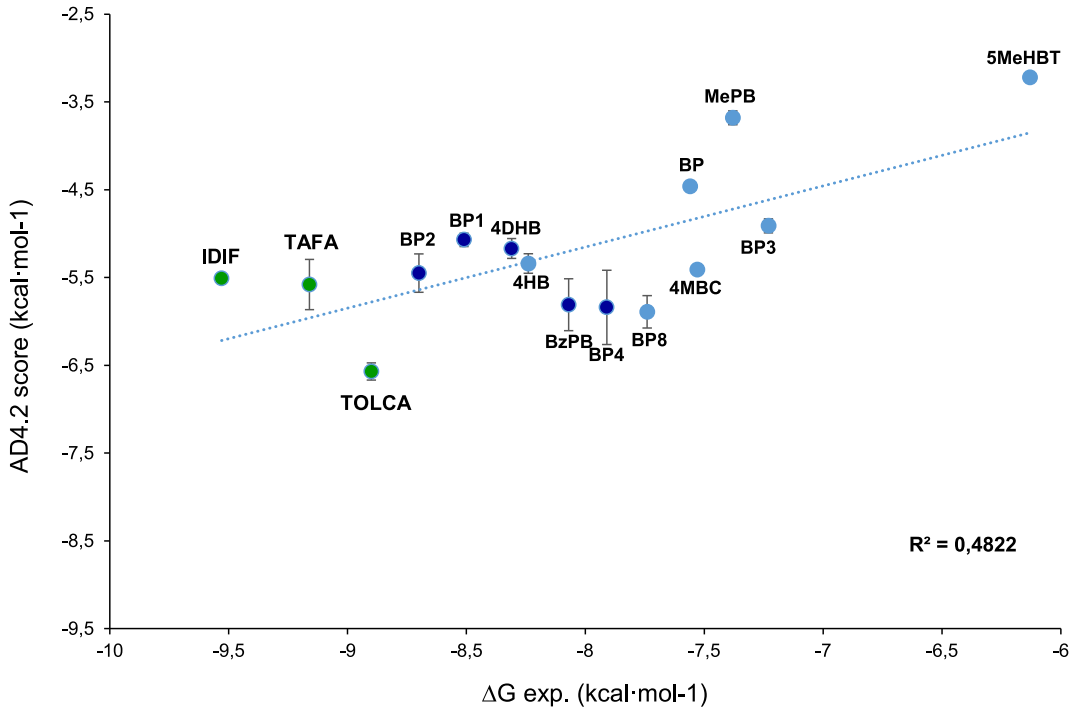

Fig. 6. Correlation between docking scores and the ITC binding energy (ΔG) of the active compounds. Reference compounds (green), active compounds with good energy binding (dark blue), and compounds with weak interaction (light blue). (For interpretation of the references to colour in this figure legend, the reader is referred to the Web version of this article.)

plasma. Their accumulation could subsequently increase the risk for developmental disorders.

We have documented the binding of some organic UVFs to TTR. Thus, attention must be given to investigate the possible adverse effects induced by binding to TTR. By previous *in vivo* studies in mice, we have proved that the formation of a complex between TTR and the ligand IDIF, can enhance the BBB permeability (Ríos et al., 2019). Consequently, we here envisaged another potentially harmful consequence stemming from the ability of TTR to cross the BBB or the placenta, enabling these compounds to surpass these important physiological barriers, thus potentially accumulating in vulnerable organs.

Pre- and postnatal exposure to environmental contaminants has consequences both at birth and on health later in life, including morbidity in adulthood (Kunisue et al., 2012; Teiri et al., 2021). Epidemiological studies with environmental contaminants of this type are still very scarce. BP-type UVFs have been detected in paired maternal and fetal samples and in paired urine and blood samples. It has been confirmed that organic UVFs and PBs accumulate in placenta (Valle--Sistac et al., 2016) and can cross the placenta to fetuses (Li et al., 2021). Moreover, UVFs and PBs have been found to bioaccumulate in breast milk (Molins-Delgado et al., 2018b). Transplacental transfer and breastfeeding are the main transport routes of organic contaminants reaching into children at the beginning of life. Information on the transport mechanism of environmental compounds across placental barrier remains limited. In the last years, the number of studies investigating transplacental transfer efficiencies of environmental contaminants is increasing (Zhang et al., 2021; Wang et al., 2021; Appel et al., 2022; Ma et al., 2022), but the mechanism still remains poorly understood. Future studies are essential to investigate the role of transporters as TTR in the transplacental transfer of these contaminants after prenatal exposure. The results presented in this paper are meaningful to evaluate the health risk induced by these compounds and their impact in the developmental neurotoxicity in humans.

Credit author statement

The manuscript was written through contributions of all authors. All authors have given approval to the final version of the manuscript. Ellen Y. Cotrina and Ângela Oliveira: Laboratory and data analysis, Xevi Biarnés: computational studies, and Jordi Llop, Jordi Quintana, Xevi Biarnés, Isabel Cardoso, M. Silvia Diaz-Cruz and Gemma Arsequell: Conceptualization, Laboratory and Data analysis, writing – review & editing.

Funding

Fundació Marató de TV3 (neurodegenerative diseases call, project reference: 20140330-31-32-33-34, http://www.ccma.cat/tv3/marato/en/projectes-financats/2013/212/).

Notes

Dedicated to Dr. Gregorio Valencia.

Declaration of competing interest

The authors declare that they have no known competing financial interests or personal relationships that could have appeared to influence the work reported in this paper.

Data availability

No data was used for the research described in the article.

Acknowledgments

I. Cardoso works under the Investigator FCT Program which is financed by national funds through FCT and co-financed by ESF through HPOP, type 4.2 - Promotion of Scientific Employment. IQAC-CSIC acknowledges a contract to Ellen Y. Cotrina funded by the project of

Fundació Marató de TV3 (Project ref. 20140330-31-32-33-34), Spain and a contract from Ford España - Fundación Apadrina la Ciencia. G. Arsequell acknowledges Dr. Rafel Prohens from Unitat de Polimorfisme i Calorimetria, Centres Científics i Tecnològics (University of Barcelona) for his supervision and assistance in ITC studies, and acknowledges Prof. Antoni Planas (IQS-URL) for full support on the TTR production. X. Biarnés acknowledges support from the Generalitat de Catalunya (2017 SGR 727, GQBB, Grup de Química Biològica i Biotecnologia) and M.S. Díaz-Cruz acknowledges support from the Generalitat de Catalunya (2017 SGR 01404, ENFOCHEM, Water, Environmental and Food Chemistry).

Appendix A. Supplementary data

Supplementary data to this article can be found online at https://doi.org/10.1016/j.envres.2022.114836.

References

Almeida, M.R., Alves, I.L., Terazaki, H., Ando, Y., Saraiva, M.J., 2000. Comparative studies of two transthyretin variants with protective effects on familial amyloidotic polyneuropathy: TTR R104H and TTR T119M. Biochem. Biophys. Res. Commun. 270, 1024–1028. https://doi.org/10.1006/bbrc.2000.2554.

Alonso, M.B., Feo, M.L., Corcellas, C., Gago-Ferrero, P., Bertozzi, C.P., Marigo, J., Flach, L., Meirelles, A.C.O., Carvalho, V.L., Azevedo, A.F., Torres, J.P., Lailson-Brito, J., Malm, O., Diaz-Cruz, M.S., Eljarrat, E., Barceló, D., 2015. Toxic heritage: maternal transfer of pyrethroid insecticides and sunscreen agents in dolphins from Brazil. Environ. Pollut. 207, 391–402. https://doi.org/10.1016/j.envpol.2015.09.039. Epub 2015 Nov 2.

Ao, J., Yuan, T., Gu, J., Ma, Y., Shen, Z., Tian, Y., Shi, R., Zhou, W., Zhang, J., 2018. Organic UV filters in indoor dust and human urine: a study of characteristics, sources, associations and human exposure. Sci. Total Environ. 640–641, 1157–1164. https://doi.org/10.1016/j.scitotenv.2018.05.367. Epub 2018 Jun 7.

Appel, M., Forsthuber, M., Ramos, R., Widhalm, R., Granitzer, S., Uhl, M., Hengstschläger, M., Stamm, T., Gundacker, C., 2022. The transplacental transfer efficiency of per- and polyfluoroalkyl substances (PFAS): a first meta-analysis. J. Toxicol. Environ. Health B Crit. Rev. 25 (1), 23–42. https://doi.org/10.1080/10937404.2021.2009946.Epub2021.Dec.20.

BCC research, 2022. Sunscreen Ingredients: Global Market to 2026. https://www.bccresearch.com/market-research/chemicals/sunscreen-ingredients-market.html.

Bell, L.J., Ucharm, G., Patris, S., Diaz-Cruz, M.S., Serra Roig, M.P., Dawson, M.N., 2017. Sunscreen Pollution Analysis in Jellyfish Lake Coral Reef Research Foundation Palau (Final report). https://coralreefpalau.org/wp-content/uploads/2017/10/CRRF-UNESCO-Sunscreen-in-Jellyfish-Lake-no.2732.pdf.

Bezerra, F., Saraiva, M.J., Almeida, M.R., 2020. Modulation of the mechanisms driving transthyretin amyloidosis. Front. Mol. Neurosci. 13, 592644 https://doi.org/10.3389/fnmol.2020.592644, 10.3389/fnmol.2020.592644.

Boberg, J., Taxvig, C., Christiansen, S., Hass, U., 2010. Possible endocrine disrupting effects of parabens and their metabolites. Reprod. Toxicol. 30, 301–312. https://doi.org/10.1016/j.reprotox.2010.03.011.

Bradford, M.M., 1976. A rapid and sensitive method for the quantitation of microgram quantities of protein utilizing the principle of protein-dye binding. Anal. Biochem. 72, 248–254. https://doi.org/10.1006/abio.1976.9999.

Bulawa, C.E., Connelly, S., Devit, M., Wang, L., Weigel, C., Fleming, J.A., Packman, J., Powers, E.T., Wiseman, R.L., Foss, T.R., Wilson, I.A., Kelly, J.W., Labaudinière, R., 2012. Tafamidis, a potent and selective transthyretin kinetic stabilizer that inhibits the amyloid cascade. Proc. Natl. Acad. Sci. U.S.A. 109, 9629–9634. https://doi.org/10.1073/pnas.1121005109. Epub 2012 May 29.

Carstensen, L., Beil, S., Börnick, H., Stolte, S., 2022. Structure-related endocrine-disrupting potential of environmental transformation products of benzophenone-type UV filters: a review. J. Hazard Mater. 430, 128495 https://doi.org/10.1016/j.jhazmat.2022.128495. Epub 2022 Feb 17.

Cotrina, E.Y., Vilà, M., Nieto, J., Arsequell, G., Planas, A., 2020a. Preparative scale production of recombinant human transthyretin for biophysical studies of protein-ligand and protein-protein interactions. Int. J. Mol. Sci. 21, 9640. https://doi.org/10.3390/ijms21249640, 10.3390/ijms21249640.

Cotrina, E.Y., Gimeno, A., Llop, J., Jiménez-Barbero, J., Quintana, J., Valencia, G., Cardoso, I., Prohens, R., Arsequell, G., 2020b. Calorimetric studies of binary and ternary molecular interactions between transthyretin, aβ peptides, and small-molecule chaperones toward an alternative strategy for alzheimer's disease drug discovery. J. Med. Chem. 63 (6), 3205–3214. https://doi.org/10.1021/acs.jmedchem.9b01970.

Cotrina, E.Y., Blasi, D., Vilà, M., Planas, A., Abad-Zapatero, C., Centeno, N.B., Quintana, J., Arsequell, G., 2020c. Optimization of kinetic stabilizers of tetrameric transthyretin: a prospective ligand efficiency-guided approach. Bioorg. Med. Chem. 28 (23), 115794 https://doi.org/10.1016/j.bmc.2020.115794.

Cotrina, E.Y., Oliveira, Â., Leite, J.P., Llop, J., Gales, L., Quintana, J., Cardoso, I., Arsequell, G., 2021. Repurposing benzbromarone for familial amyloid polyneuropathy: a new transthyretin tetramer stabilizer. Int. J. Mol. Sci. 21 (19), 7166. https://doi.org/10.3390/ijms21197166.

de Miranda, L.L.R., Harvey, K.E., Ahmed, A., Harvey, S.C., 2021. UV-filter pollution: current concerns and future prospects. Environ. Monit. Assess. 193 (12), 840. https://doi.org/10.1007/s10661-021-09626-6, 10.1007/s10661-021-09626-6. PMID: 34822005.

Díaz-Cruz, M.S., Barceló, D. (Eds.), 2015. Personal care products in the aquatic environment. In: Barceló, D., Kostianoy, A.G. (Eds.), 2015, The Handbook of Environmental Chemistry, 36. Springer International Publishing, London.

EU, 2009. EU regulation (EC) No 1223/2009 of the European Parliament and of the Council of 30 November 2009 on cosmetic products (recast.). Off. J. Eur. Union L 342. EU, 2021. Cosmetic ingredient database (Cosing). List of UV filters allowed in cosmetic products. Annex VI. http://ec.europa.eu/growth/tools-databases/cosing/pdf/COSING_Annex%20VI_v2.pdf.

Hamers, T., Kortenkamp, A., Scholze, M., Molenaar, D., Cenijn, P.H., Weiss, J.M., 2020. Transthyretin-binding activity of complex mixtures representing the composition of thyroid-hormone disrupting contaminants in house dust and human serum. Environ. Health Perspect. 128 (1), 17015 https://doi.org/10.1289/EHP5911, 10.1289/EHP5911 Epub 2020 Jan 31.

Hill, K.L., Mortensen, Å.K., Teclechiel, D., Willmore, W.G., Sylte, I., Jenssen, B.M., Letcher, R.J., 2018a. In vitro and in silico competitive binding of brominated polyphenyl ether contaminants with human and gull thyroid hormone transport proteins. Environ. Sci. Technol. 52, 1533–1541.

Hill, K.L., Hamers, T., Kamstra, J.H., Willmore, W.G., Letcher, R.J., 2018b. Organophosphate triesters and selected metabolites enhance binding of thyroxine to human transthyretin *in vitro*. Toxicol. Lett. 285, 87–93. https://doi.org/10.1016/j.toxlet.2017.12.030. Epub 2018 Jan 3.

Hu, P., Chen, X., Whitener, R.J., Boder, E.T., Jones, J.O., Porollo, A., Chen, J., Zhao, L., 2013a. Effects of parabens on adipocyte differentiation. Toxicol. Sci. 131, 56–70. https://doi.org/10.1093/toxsci/kfs262.

Hu, Y., Zhang, Z., Sun, L., Zhu, D., Liu, Q., Jiao, J., Li, J., Qi, M., 2013b. The estrogenic effects of benzylparaben at low doses based on uterotrophic assay in immature SD rats. Food Chem. Toxicol. 53, 69–74. https://doi.org/10.1016/j.fct.2012.11.043.

Huang, Y., Law, J.C., Lam, T.K., Leung, K.S., 2021. Risks of organic UV filters: a review of environmental and human health concern studies. Sci. Total Environ. 755 (Pt 1), 142486 https://doi.org/10.1016/j.scitotenv.2020.142486.

Humphrey, W., Dalke, A., Schulten, K., 1996. Vmd - visual molecular Dynamics. J. Mol. Graph. 14, 33–38. https://doi.org/10.1016/0263-7855(96)00018-5.

Iakovleva, I., Begum, A., Brännström, K., Wijsekera, A., Nilsson, L., Zhang, J., Andersson, P.L., Sauer-Eriksson, A.E., Olofsson, A., 2016. Tetrabromobisphenol A is an efficient stabilizer of the transthyretin tetramer. PLoS One 11 (4), e0153529. https://doi.org/10.1371/journal.pone.0153529. Apr 19.

Koren, G., Ornoy, A., 2018. The role of the placenta in drug transport and fetal drug exposure. Expet Rev. Clin. Pharmacol. 11, 373–385. https://doi.org/10.1080/17512433.2018.1425615. Epub 2018 Jan 16.

Krause, M., Frederiksen, H., Sundberg, K., Jørgensen, F.S., Jensen, L.N., Nørgaard, P., Jørgensen, C., Ertberg, P., Juul, A., Drzewiecki, K.T., Skakkebaek, N.E., Andersson, A.M., 2018. Presence of benzophenones commonly used as UV filters and absorbers in paired maternal and fetal samples. Environ. Int. 110, 51–60. https://doi.org/10.1016/j.envint.2017.10.005.

Kunisue, T., Chen, Z., Buck Louis, G.M., Sundaram, R., Hediger, M.L., Sun, L., Kannan, K., 2012. Urinary concentrations of benzophenone-type UV filters in U.S. women and their association with endometriosis. Environ. Sci. Technol. 46, 4624–4632. https://doi.org/10.1021/es204415a. Epub 2012 Mar 29.

Landers, K.A., Mortimer, R.H., Richard, K., 2013. Transthyretin and the human placenta. Placenta 34, 513–517. https://doi.org/10.1016/j.placenta.2013.04.013. Epub 2013 May 9.

Lans, M.C., Klasson-Wehler, E., Willemsen, M., Meussen, E., Safe, S., Brouwer, A., 1993. Structure-dependent, competitive interaction of hydroxy-polychlorobiphenyls, -dibenzo-p-dioxins and -dibenzofurans with human transthyretin. Chem. Biol. Interact. 88, 7–21. https://doi.org/10.1016/0009-2797(93)90081-9.

Li, J., Sun, X., Xu, J., Tan, H., Zeng, E.Y., Chen, D., 2021. Transplacental transfer of environmental chemicals: roles of molecular descriptors and placental transporters. Environ. Sci. Technol. 55 (1), 519–528. https://doi.org/10.1021/acs.est.0c06778. Epub 2020 Dec 9.

Liu, X., Fang, M., Xu, F., Chen, D., 2019. Characterization of the binding of per- and poly-fluorinated substances to proteins: a methodological review. TrAC, Trends Anal. Chem. 116, 177–185. https://doi.org/10.1016/j.trac.2019.05.017.

Ma, D., Lu, Y., Liang, Y., Ruan, T., Li, J., Zhao, C., Wang, Y., Jiang, G., 2022. A critical review on transplacental transfer of per- and polyfluoroalkyl substances: prenatal exposure levels, characteristics, and mechanisms. Environ. Sci. Technol. 56 (10), 6014–6026. https://doi.org/10.1021/acs.est.1c01057. Epub 2021 Jun 18.

Mairal, T., Nieto, J., Pinto, M., Almeida, M.R., Gales, L., Ballesteros, A., Barluenga, J., Pérez, J.J., Vázquez, J.T., Centeno, N.B., Saraiva, M.J., Damas, A.M., Planas, A., Arsequell, G., Valencia, G., 2009. Iodine atoms: a new molecular feature for the design of potent transthyretin fibrillogenesis inhibitors. PLoS One 4, e4124. https://doi.org/10.1371/journal.pone.0004124. Epub 2009 Jan 6.

Mao, J.F., Li, W., Ong, C.N., He, Y., Jong, M.C., Gin, K.Y., 2022. Assessment of human exposure to benzophenone-type UV filters: a review. Environ. Int. 167, 107405 https://doi.org/10.1016/j.envint.2022.107405.

Marchesini, G.R., Meulenberg, E., Haasnoot, W., Mizuguchi, M., Irth, H., 2006. Biosensor recognition of thyroid-disrupting chemicals using transport proteins. Anal. Chem. 78 (4), 1107–1114. https://doi.org/10.1021/ac051399i.

Marchesini, G.R., Meimaridou, A., Haasnoot, W., Meulenberg, E., Albertus, F., Mizuguchi, M., Takeuchi, M., Irth, H., Murk, A.J., 2008. Biosensor discovery of thyroxine transport disrupting chemicals. Toxicol. Appl. Pharmacol. 232 (1), 150–160. https://doi.org/10.1016/j.taap.2008.06.014.

McKinnon, B., Li, H., Richard, K., Mortimer, R., 2005. Synthesis of thyroid hormone binding proteins transthyretin and albumin by human trophoblast. J. Clin. Endocrinol. Metab. 90, 6714–6720. https://doi.org/10.1210/jc.2005-0696. Epub 2005 Sep. 13.

Meeker, J.D., Yang, T., Ye, X., Calafat, A.M., Hauser, R., 2011. Urinary concentrations of parabens and serum hormone levels, semen quality parameters, and sperm DNA damage. Environ. Health Perspect. 119 (2), 252–257. https://doi.org/10.1289/ehp.1002238.

Meerts, I.A., van Zanden, J.J., Luijks, E.A., van Leeuwen-Bol, I., Marsh, G., Jakobsson, E., Bergman, A., Brouwer, A., 2000. Potent competitive interactions of some brominated flame retardants and related compounds with human transthyretin in vitro. Toxicol. Sci. 56 (1), 95–104. https://doi.org/10.1093/toxsci/56.1.95.

Molecular Operating Environment (Moe), 2019. 01, Chemical Computing Group ULC, 1010, 2R7. Canada, H3A, Montreal, QC, p. 2021. Sherbooke St. West, Suite #910.

Molins-Delgado, D., Máñez, M., Andreu, A., Hiraldo, F., Eljarrat, E., Barceló, D., Díaz-Cruz, M.S., 2017. A potential new threat to wild life: presence of UV filters in bird eggs from a preserved area. Environ. Sci. Technol. 51, 10983–10990. https://doi.org/10.1021/acs.est.7b03300.

Molins-Delgado, D., Muñoz, R., Nogueira, S., Alonso, M.B., Torres, J.P., Malm, O., Ziolli, R.L., Hauser-Davis, R.A., Eljarrat, E., Barceló, D., Díaz-Cruz, M.S., 2018a. Occurrence of organic UV filters and metabolites in lebranche mullet (Mugil liza) from Brazil. Sci. Total Environ. 618, 451–459. https://doi.org/10.1016/j.scitotenv.2017.11.033.

Molins-Delgado, D., Olmo-Campos, M.D.M., Valeta-Juan, G., Pleguezuelos-Hernández, V., Barceló, D., Díaz-Cruz, M.S., 2018b. Determination of UV filters in human breast milk using turbulent flow chromatography and babies' daily intake estimation. Environ. Res. 161, 532–539. https://doi.org/10.1016/j.envres.2017.11.033.

Morris, G.M., Huey, R., Lindstrom, W., Sanner, M.F., Belew, R.K., Goodsell, D.S., Olson, A.J., 2009. Autodock4 and AutoDockTools4: automated docking with selective receptor flexiblity. J. Comput. Chem. 16, 2785–2791. https://doi.org/10.1002/jcc.21256.

Ouyang, X., Froment, J., Leonards, P.E.G., Christensen, G., Tollefsen, K.E., de Boer, J., Thomas, K.V., Lamoree, M.H., 2017. Miniaturization of a transthyretin binding assay using a fluorescent probe for high throughput screening of thyroid hormone disruption in environmental samples. Chemosphere 171, 722–728. https://doi.org/10.1016/j.chemosphere.2016.12.119. Epub 2016 Dec 23.

Pappa, T., Refetoff, S., 2017. Thyroid Hormone Transport Proteins: Thyroxine-Binding Globulin, Transthyretin, and Albumin, Reference Module in Neuroscience and Biobehavioral Psychology. Elsevier, Amsterdam, The Netherlands. https://doi.org/10.1016/B978-0-12-809324-5.03494-5.

Pomierny, B., Krzyżanowska, W., Broniowska, Ż., Strachm, B., Bystrowska, B., Starek-Świechowicz, B., Maciejska, A., Skórkowska, A., Wesołowska, J., Walczak, M., Budziszewska, B., 2019. Benzophenone-3 passes through the blood-brain barrier, increases the level of extracellular glutamate and induces apoptotic processes in the hippocampus and frontal cortex of rats. *Toxicol Sci.* Jul 31. https://doi.org/10.1093/toxsci/kfz160 kfz160 (Epub ahead of print).

Purkey, H.E., Palaninathan, S.K., Kent, K.C., Smith, C., Safe, vS.H., Sacchettini, J.C., Kelly, J.W., 2004. Hydroxylated polychlorinated biphenyls selectively bind transthyretin in blood and inhibit amyloidogenesis: rationalizing rodent PCB toxicity. Chem. Biol. 11, 1719–1728. https://doi.org/10.1016/j.chembiol.2004.10.009.

Razavi, H., Palaninathan, S.K., Powers, E.T., Wiseman, R.L., Purkey, H.E., Mohamedmohaideen, N.N., Deechongkit, S., Chiang, K.P., Dendle, M.T.A., Sacchettini, J.C., Kelly, J.W., 2003. Benzoxazoles as transthyretin amyloid fibril inhibitors: synthesis, evaluation, and mechanism of action. Angew. Chem. Int. Ed. 115, 2864–2867. https://doi.org/10.1002/anie.200351179.

Ren, X.M., Guo, L.H., 2012. Assessment of the binding of hydroxylated polybrominated diphenyl ethers to thyroid hormone transport proteins using a site-specific fluorescence probe. Environ. Sci. Technol. 46, 4633–4640. https://doi.org/10.1021/es2046074. Epub 2012 Apr 6.

Ren, X.M., Qin, W.P., Cao, L.Y., Zhang, J., Yang, Y., Wan, B., Guo, L.H., 2016. Binding interactions of perfluoroalkyl substances with thyroid hormone transport proteins and potential toxicological implications. Toxicology 366–367, 32–42. https://doi.org/10.1016/j.tox.2016.08.011.

Richardson, S.J., 2009. Evolutionary changes to transthyretin: evolution of transthyretin biosynthesis. FEBS J. 276 (19), 5342–5356. https://doi.org/10.1111/j.1742-4658.2009.07244.x.

Ríos, X., Gómez-Vallejo, V., Martín, A., Cossío, U., Morcillo, M.Á., Alemi, M., Cardoso, I., Quintana, J., Jiménez-Barbero, J., Cotrina, E.Y., Valencia, G., Arsequell, G., Llop, J., 2019. Radiochemical examination of transthyretin (TTR) brain penetration assisted by iododiflunisal, a TTR tetramer stabilizer and a new candidate drug for AD. Sci. Rep. Sep 20 (1), 13672. https://doi.org/10.1038/s41598-019-50071-w, 10.1038/s41598-019-50071-w.

Sabzevari, N., Qiblawi, S., Norton, S.A., Fivenson, D., 2021. Sunscreens: UV filters to protect us: Part 1: changing regulations and choices for optimal sun protection. Int. J. Womens Dermatol. 7, 28–44. https://doi.org/10.1016/j.ijwd.2020.05.017.

Sant'Anna, R., Gallego, P., Robinson, L.Z., Pereira-Henriques, A., Ferreira, N., Pinheiro, F., Esperante, S., Pallares, I., Huertas, O., Almeida, M.R., Reixach, N., Insa, R., Velazquez-Campoy, A., Reverter, D., Reig, N., Ventura, S., 2016. Repositioning tolcapone as a potent inhibitor of transthyretin amyloidogenesis and associated cellular toxicity. Nat. Commun. 7, 10787 https://doi.org/10.1038/ncomms10787.

Savage, J.H., Matsui, E.C., Wood, R.A., Keet, C.A., 2012. Urinary levels of triclosan and parabens are associated with aeroallergen and food sensitization. J. Allergy Clin. Immunol. 130, 453–460. https://doi.org/10.1016/j.jaci.2012.05.006 e457.

Shaath, N.A., 2010. Ultraviolet filters. Photochem. Photobiol. Sci. 9, 464–469. https://doi.org/10.1039/b9pp00174c.

Song, S., He, Y., Huang, Y., Huang, X., Guo, Y., Zhu, H., Kannan, K., Zhang, T., 2020. Occurrence and transfer of benzophenone-type ultraviolet filters from the pregnant women to fetuses. Sci. Total Environ. 726, 138503 https://doi.org/10.1016/j.scitotenv.2020.138503, 10.1016/j.scitotenv.2020.138503 Epub 2020 Apr 12.

Sunyer-Caldú, A., Peiró, A., Díaz, M., Ibáñez, L., Gago-Ferrero, P., Díaz-Cruz, M.S., 2021. Development of a sensitive analytical method for the simultaneous analysis of benzophenone-type UV filters and paraben preservatives in umbilical cord blood. MethodsX 8, 1013. https://doi.org/10.1016/j.mex.2021.101307.

Teiri, H., Samaei, M.R., Dehghani, M., Azhdarpoor, A., Hajizadeh, Y., Mohammadi, F., Kelishadi, R., 2021. The association of prenatal exposure to benzophenones with gestational age and offspring size at birth. *Environ. Sci. Pollut. Res. Int.* Nov 26, 1–14. https://doi.org/10.1007/s11356-021-17634-9. Epub 2021 Nov 26.

Tsui, M.M.P., Lam, J.C.W., Ng, T.Y., Ang, P.O., Murphy, M.B., Lam, P.K.S., 2017. Occurrence, distribution, and fate of organic UV filters in coral communities. Environ. Sci. Technol. 51, 4182–4190. https://doi.org/10.1021/acs.est.6b05211.

Valle-Sistac, J., Molins-Delgado, D., Diaz, M., Ibanez, L., Barcelo, D., Diaz-Cruz, M.S., 2016. Determination of parabens and benzophenone-type UV filters in human placenta. First description of the existence of benzyl paraben and benzophenone-4. Environ. Int. 88, 243–249. https://doi.org/10.1016/j.envint.2015.12.034. Epub 2016 Jan 11.

van der Meer, T.P., Artacho-Cordón, F., Swaab, D.F., Struik, D., Makris, K.C., Wolffenbuttel, B.H.R., Frederiksen, H., van Vliet-Ostaptchouk, J.V., 2017. Distribution of non-persistent endocrine disruptors in two different regions of the human brain. Int. J. Environ. Res. Publ. Health 14 (9), 1059. https://doi.org/10.3390/ijerph14091059, 10.3390/ijerph14091059. PMID: 28902174, PMCID: PMC5615596.

Vieira, M., Saraiva, M.J., 2014. Transthyretin: a multifaceted protein. Biomol. Concepts 5, 45–54. https://doi.org/10.1515/bmc-2013-0038.

Wang, X., Chen, P., Zhao, L., Zhu, L., Wu, F., 2021. Transplacental behaviors of organophosphate tri- and diesters based on paired human maternal and cord whole blood: efficiencies and impact factors. Environ. Sci. Technol. 55, 3091–3100. https://doi.org/10.1021/acs.est.0c06095. Epub 2021 Jan 4.

Ward, W.H., Holdgate, G.A., 2001. Isothermal titration calorimetry in drug discovery. Prog. Med. Chem. 38, 309–376. https://doi.org/10.1016/s0079-6468(08)70097-3.

Weiss, J.M., Andersson, P.L., Lamoree, M.H., Leonards, P.E., van Leeuwen, S.P., Hamers, T., 2009. Competitive binding of poly- and perfluorinated compounds to the thyroid hormone transport protein transthyretin. Toxicol. Sci. 109, 206–216. https://doi.org/10.1093/toxsci/kfp055. Epub 2009 Mar 17.

Weiss, J.M., Andersson, P.L., Zhang, J., Simon, E., Leonards, P.E., Hamers, T., Lamoree, M.H., 2015. Tracing thyroid hormone-disrupting compounds: database compilation and structure-activity evaluation for an effect-directed analysis of sediment. Anal. Bioanal. Chem. 407, 5625–5634. https://doi.org/10.1007/s00216-015-8736-9. Epub 2015 May 19.

Wojtczak, A., Neumann, P., Cody, V., 2001. Structure of a new polymorphic monoclinic form of human transthyretin at 3 A resolution reveals a mixed complex between unliganded and T4-bound tetramers of TTR. Acta Crystallogr. D Biol. Crystallogr. 57 (Pt 7), 957–967. https://doi.org/10.1107/s0907444901006047. Epub 2001 Jun 21.

World Health Organization (Who), 2022. Ultraviolet (UV) Radiation. https://www.who.int/data/gho/data/themes/topics/topic-details/GHO/ultraviolet-(uv)-radiation.

Xin, Y., Ren, X.M., Ruan, T., Li, C.H., Guo, L.H., Jiang, G., 2018. Chlorinated polyfluoroalkylether sulfonates exhibit similar binding potency and activity to thyroid hormone transport proteins and nuclear receptors as perfluorooctanesulfonate. Environ. Sci. Technol. 52 (16), 9412–9418. https://doi.org/10.1021/acs.est.8b01494.

Zhang, J., Kamstra, J.H., Ghorbanzadeh, M., Weiss, J.M., Hamers, T., Andersson, P.L., 2015. In silico approach to identify potential thyroid hormone disruptors among currently known dust contaminants and their metabolites. Environ. Sci. Technol. 49, 10099–100107. https://doi.org/10.1021/acs.est.5b01742. Epub 2015 Aug 6.

Zhang, J., Begum, A., Brännström, K., Grundström, C., Iakovleva, I., Olofsson, A., Sauer-Eriksson, A.E., Andersson, P.L., 2016. Structure-based virtual screening protocol for in silico identification of potential thyroid disrupting chemicals targeting transthyretin. Environ. Sci. Technol. 50, 11984–11993. https://doi.org/10.1021/acs.est.6b02771. Epub 2016 Oct 10.

Zhang, X., Cheng, X., Lei, B., Zhang, G., Bi, Y., Yu, Y., 2021. A review of the transplacental transfer of persistent halogenated organic pollutants: transfer characteristics, influential factors, and mechanisms. Environ. Int. 146, 106224 https://doi.org/10.1016/j.envint.2020.106224.Epub202.Nov.1.